d Collection

공학석사 학위논문

Evaluation of Dynamic Earth Pressure acting on Piles in Liquefiable Soils Using 1g shaking table tests

1g 진동대 실험을 이용한 액상화 지반에서 말뚝에 작용하는 동적 토압 평가

2012년 8월

서울대학교 대학원

건 설 환 경 공 학 부

정 인 우

Evaluation of Dynamic Earth Pressure acting on Piles in Liquefied Soil Using 1g shaking table tests

1g 진동대 실험을 이용한 액상화 지반에서 말뚝에 작용하는 동적 토압 평가

지도 교수 김 명 모

이 논문을 공학석사 학위논문으로 제출함
2012년 8월

서울대학교 대학원
건 설 환 경 공 학 부
정 인 우

정인우의 공학석사 학위논문을 인준함
2012년 8월

위 원 장 _____ 정 충 기 _____ (인)

부위원장 _____ 김 명 모 _____ (인)

위   원 _____ 박 준 범 _____ (인)

Abstract

Evaluation of Dynamic Earth Pressure acting on Piles in Liquefied Soil using 1g shaking table tests

Jung, Inwoo

Department of Civil and Environmental Engineering

The Graduate School

Seoul National University

In this research, the dynamic earth pressure acting on piles in liquefiable soils was evaluated using 1g shaking table tests. The magnitude and distribution of the pile displacements were analyzed with various pile diameters and concentrated mass. The earth pressure acting on piles were also evaluated with depth and pile diameters in liquefiable soil. Moreover, the dynamic earth pressure acting on piles was analyzed for various concentrated mass and compared with ground displacement. It was also compared that the kinematic effect and Inertial effect qualitatively. The westergaard solution which can calculate the fluctuating component of the dynamic water force acting on quay wall was verified as a analytic method to evaluate the dynamic earth pressure acting on piles in liquefiable soils.

Keywords: Dynamic earth pressure, westergaard solution, pile diameter, liquefaction, inertial force, kinematic force, shaking table test

Student Number: 2010-23317

Contents

List of Tables

List of Figures

Chapter 1 Introduction

1.1 Background

For foundation of structures, pile foundation is widely used. Recently, pile foundation works good against not only vertical loading but lateral loading. It also has advanced to the point of good working against catastrophes such as earthquakes. However, because of reduction of soil resistance and lateral earth pressure induced from ground displacement, pile foundation often cannot resist earthquake and failed when it was installed in liquefiable ground. Especially, when ground liquefaction is occurred by earthquake, the lateral earth pressure acting on pile foundation is very important factor for safety of structure. There are several representative examples of pile foundation failure by earthquake and liquefaction such as Niigata Earthquake (1964), Kobe Earthquake (1995), and the nearest catastrophe of The Japan Earthquake.

There are two component of load which are inertial force and kinematic force acting on pile foundation when earthquake is occurred, and a lot of researches about these component of load have studied continuously. Especially, many researchers have focused on inertial force for a design of pile foundation in the past, whereas lots of researches focused on kinematic force are presented recently (Tokimatsu, 2005). However, researches about relation between inertial force and kinematic force are still lack, so continuous study about the relation and estimation method of inertial force and kinematic

force are needed.

In case of lateral dynamic earth pressure which is important factor of pile foundation safety acting on pile foundation in liquefiable ground, there is insufficient method to estimate the lateral dynamic earth pressure acting on pile foundation because of the non-linearity. In the past, Kohama and Sato (2000) suggested a method to estimate the lateral dynamic earth pressure acting on quay wall by using Westergaard solution(Westergaard, 1933), Han suggested a method to estimate the lateral dynamic earth pressure acting on pile foundation by using Westergaard solution. At first, Westergaard solution is developed for estimating dynamic water pressure. However, when the liquefaction is occurred, the dynamic earth pressure can be estimated by using Westergaard solution because that the liquefied ground behave like fluid. However, the estimation of the dynamic earth pressure acting on pile foundation is still needed to verify based on various parameter study.

1.2 Objective

Han (2006) suggested a method to estimate dynamic earth pressure acting on pile foundation in liquefied ground by using Westergaard solution applied a shape factor of pile. However, in his research, it is still needed that consideration of various parametric study, and it has limitations that lack of quantity of data for verification of equation. Therefore, in this research, properties of dynamic behavior of pile will be analyzed, the dynamic earth pressure acting on pile foundation will be estimated when liquefaction is occurred by earthquake using 1g shaking table test. Moreover, the estimation method to calculate the dynamic earth pressure acting on pile foundation in liquefied ground by using Westergaard solution will be verified based on comparison between experimental data and Westergaard solution.

Chapter 2 Previous Research

2.1 Evaluation of seismic Behavior of Piles in Liquefiable Ground by Shaking Table Tests (Han, 2006)

This thesis evaluate seismic behavior of piles in liquefiable ground by 1g shaking table test, and Chapter 5 "Analysis of force components acting on piles in liquefiable ground" was reviewed. In the figure 2.1, eight strain gauge was attached on the left pile, and four earth pressure transducer was attached on right pile. Moreover, seven pore water pressure transducer and four accelerometer was installed in the ground with depth, and LVDT was installed on the pile head. Three type of ground conditions, water, dry sand, and saturated sand, are prepared. The installed model piles are aluminum piles having a diameter of 14mm and a length of 550mm. In addition, model soil box used in this research was acryl box with a length of 194cm, a width of 44cm, and a height of 60cm. Sponges with a thickness of 5cm were attached on the both sides of the model soil box to absorb the reflective waves.
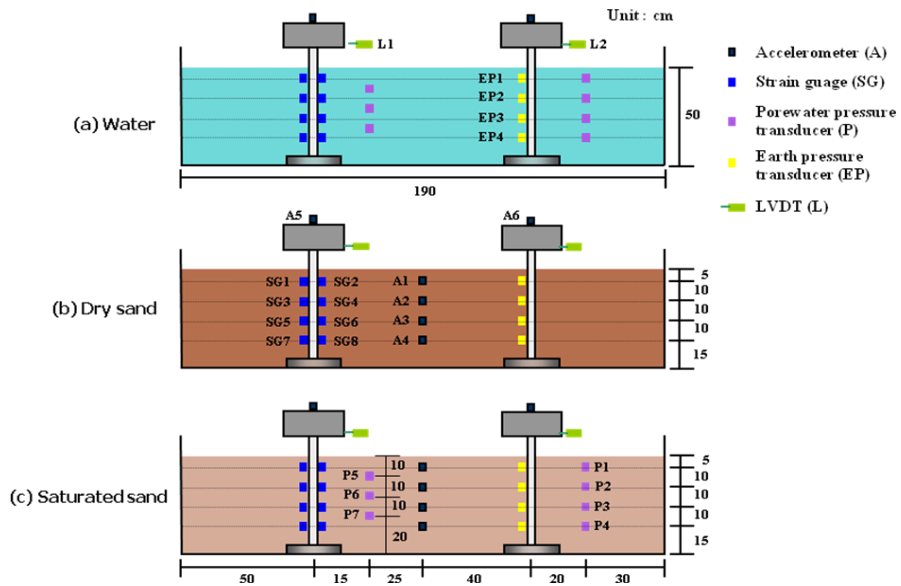
Figure 2.1 Schematic drawing of test section

In table 2.1, the test program is summarized. The tests were conducted with various ground condition, input acceleration, input frequency, relative density, and axial load.

Table 2.1 Test program

Ground condition	Input Acc. (sine wave)	Loading duration (sec)	Loading frequency (Hz)	Re-Loading frequency (Hz)	Relative density (%)	Axial load
Water	0.1g	5	10, 2, 5	-	-	0kg
	0.2g	5	10	-	-	0kg
	0.1g	5	10, 2, 5, 3	-	-	3.8kg
Dry sand	0.1g	5	10	2, 2, 5, 5	38	0kg
	0.1g	5	10	2	38	3.8kg
	0.1g	5	10, 2, 5	-	80	0kg
	0.1g	5	10, 2, 5	-	80	3.8kg
	0.2g	5	10	-	80	3.8kg
	0.1g	5	10, 2, 5	-	80	7.6kg
Saturated sand	0.2g	8	2	10	54	0kg
	0.2g	8	2	10, 10, 5	54	3.8kg
	0.2g	8	5	5, 5	54	3.8kg
	0.2g	8	10	10, 10	54	3.8kg
	0.2g	8	10	10, 10	25	0kg
	0.2g	8	5	5, 5	25	3.8kg
	0.2g	8	10	10, 10	25	3.8kg
	0.1g	8	10	10(0.2g), 10(0.2g)	25	3.8kg
	0~0.2g + 0.2g	5 + 5	10	10	25	3.8kg
	0.2g	8	10	10, 10	25	7.6kg

Figure 2.2 shows the picture which describe force component acting on pile. In this figure, inertial force is represented by axial force, and kinematic force is represented by dynamic pore water pressure and dynamic earth pressure.

In figure 2.3, the dynamic forces are divided by fluctuating component and non-fluctuating component. Therefore in this research, by using this concept, the experimental data were analyzed.
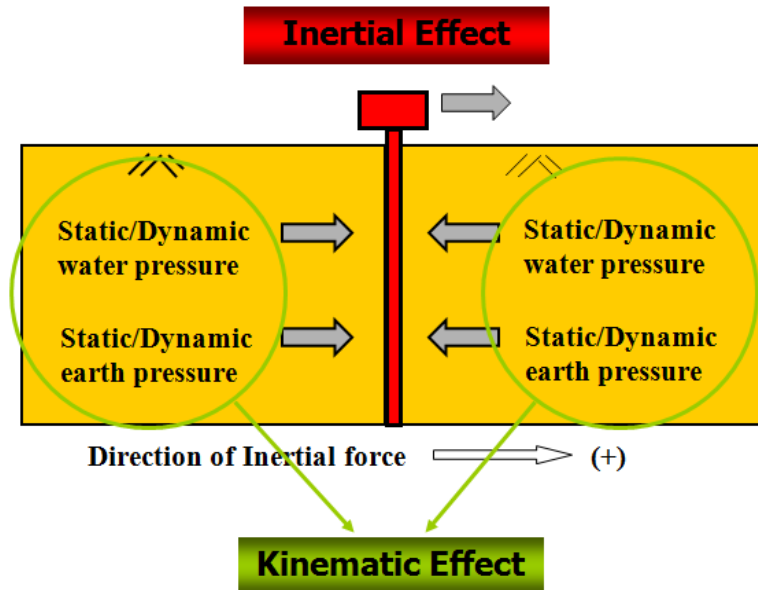
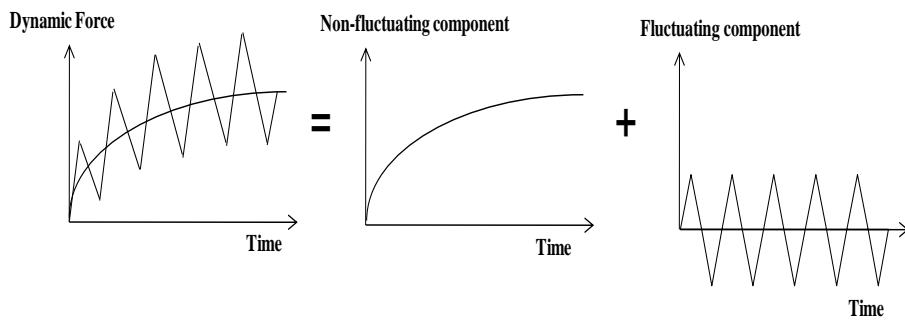Figure 2.2 Force components acting on pile

Figure 2.3   Division of fluctuating and non-fluctuating components (Kim et al., 2004)

Figure 2.4 (a), (b), (c) are graph which show maximum earth pressure acting on pile, maximum pile displacement, and maximum ground displacement according to axial load in saturated sand respectively. As shown

in Figure 2.4 (a), existence of axial load and weight of axial load cannot have influence on maximum dynamic earth pressure with depth in all cases. Moreover, in figure 2.4 (b), it also shows that maximum pile displacement has almost same tendency and magnitude regardless of axial load. Figure 2.4 (c) shows that maximum soil displacement increases with depth, and this tendency is similar to tendency of the maximum dynamic earth pressure with depth in figure 2.4 (a). Therefore, it can be inferred that the maximum dynamic earth pressure acting on piles with depth in liquefied ground is influenced kinematic force by ground displacement rather than inertial force by axial force.
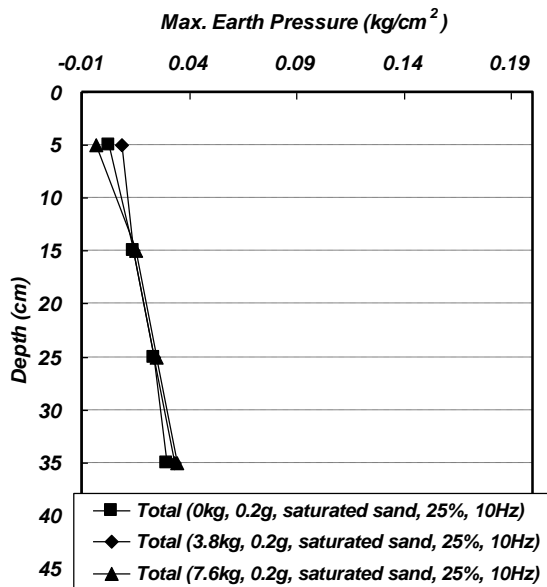
(a) Maximum earth pressure
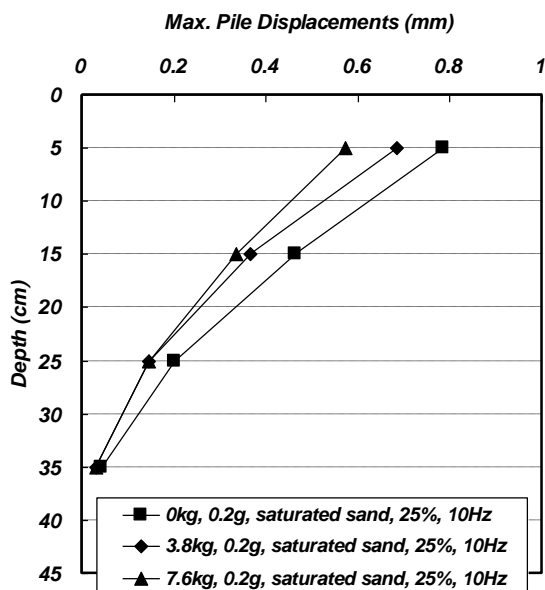
(b) Maximum pile displacement
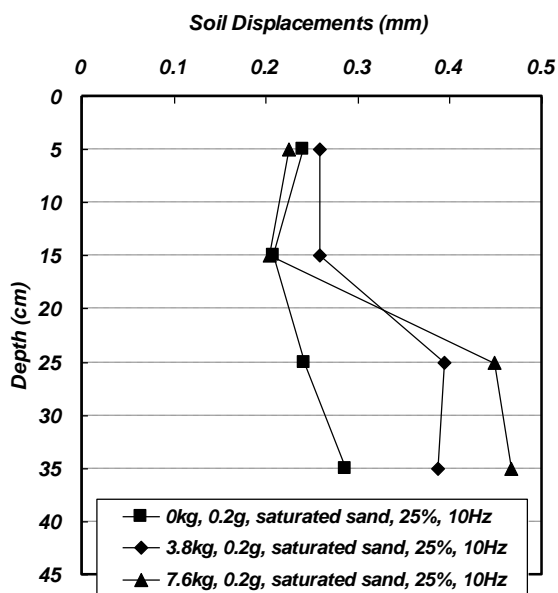
(c) Maximum soil displacement

9

Figure 2.4 Earth pressure, pile displacement, and soil displacement

according to axial load(saturated sand)

Equation (1) is modified Westergaard solution suggested by Kohama and Sato for calculating dynamic earth pressure acting on quay wall. (Kohama, 2000; Sato, 2000). The Westergaard solution is for calculating dynamic water pressure, whereas the modified Westergaard solution is for calculating the dynamic earth pressure of ground which behave like fluid by liquefaction. When the dynamic earth pressure is calculated by using modified Westergaard solution, γ_{sat} will replace γ_w in the equation. Han applied shape factor to this modified Westergaard solution, and he suggested that the method for calculating the dynamic earth pressure acting on piles.

$$q(z) = \frac{7}{8} k_h \gamma_{sat} \sqrt{H_w z}$$

$$F_{DF} = \int q(z) = \frac{7}{12} k_h \gamma_{sat} H_w^2$$

(1)

where,

q(z) : dynamic water pressure at the depth of z

F_{DF} : fluctuating component of dynamic thrust after liquefaction

γ_{sat} : saturated unit weight of soil

k_h : horizontal seismic coefficient

H_w : water depth

In figure 2.5, comparison was conducted between fluctuating component of dynamic earth pressure calculated by experimental data and Westergaard solution. As shown in figure 2.5, it was confirmed that the fluctuating component of dynamic earth pressure based on experimental data can be calculated by 50% of Westergaard solution using γ_w. Moreover, it was also confirmed that the fluctuating component of dynamic water pressure can be calculated by 20% of Westergaard solution using γ_w. It was because that the quay wall have a plane surface, whereas the pile have a curved surface, and the earth pressure acting on piles reduced. Therefore, it is estimated that the ratio of reduction of earth pressure is 50% based on shape of pile, and it can be calculated the fluctuating component of dynamic earth pressure acting on piles in liquefied ground.
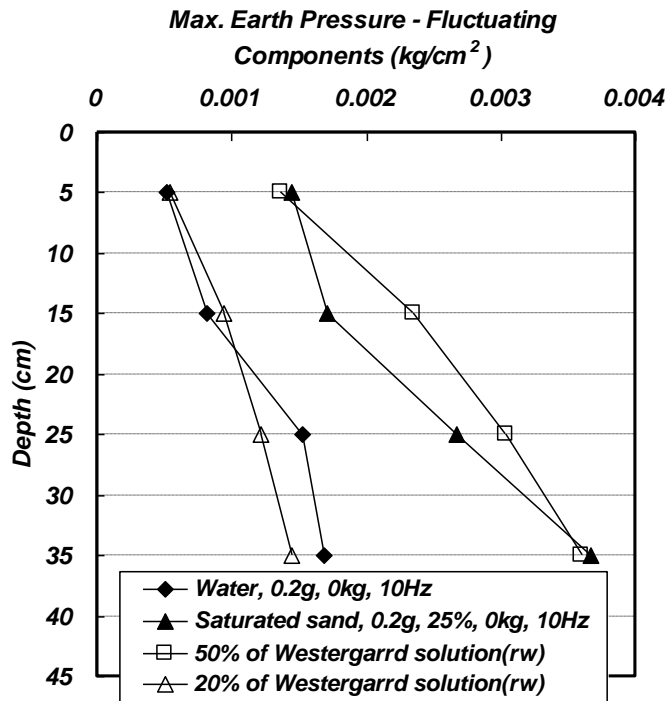
Figure 2.5 Comparison of dynamic earth pressure and westergaard solution

Chapter 3 Test Set-Up and Programs

In this research, four 1g shaking table tests were conducted with various upper mass of pile head and pile diameter. As shown in figure 3.2, dimensions of soil box are 192cm by 44cm rectangle, and its height is 60cm. Moreover, the soil box is made of acryl soil box. The dynamic earth pressure acting on piles are evaluated with same test conditions such as input acceleration, input frequency, and relative density of saturated sand are applied to all of test cases. The reason that ground condition is saturated sand is for estimation of the effect of liquefaction to the earth pressure acting on pile foundation when the liquefaction was occurred by earthquake.

In all of test cases, 1g shaking table located at Hyundai Institute of Construction Technology is used. Dimensions of 1g shaking table are 2m by 2m square biaxial shaking table, maximum specimen weigh is 5ton, and maximum frequency is 50Hz. The detail specifications of shaking table are summarized in table 3.1.
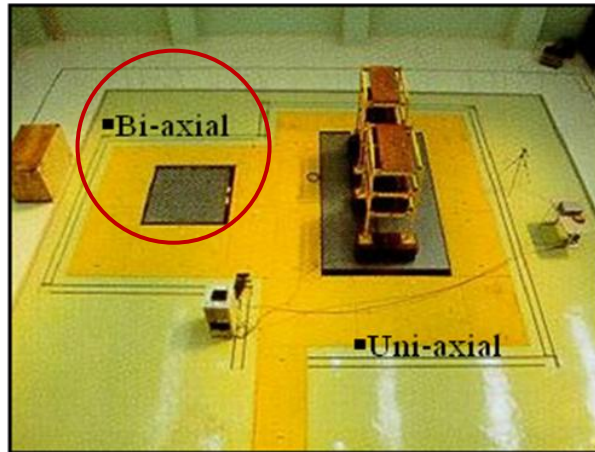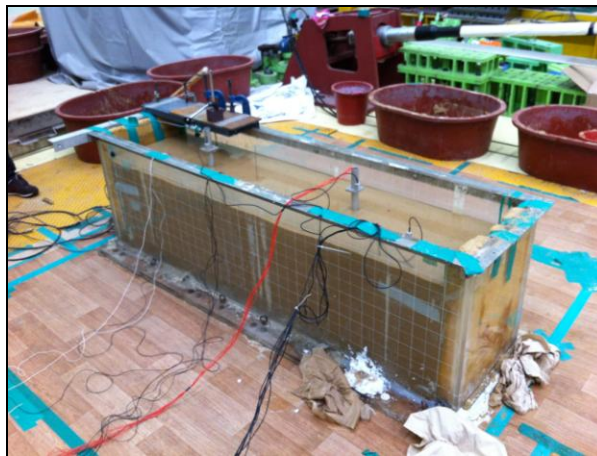
Figure 3.1 1g shaking table

Figure 3.2 Model soil box

Table 3.1 Specifications of shaking table

Specifications	Biaxial table
Dimension	2m × 2m
Max. Specimen weight	5 ton
Table Mass	2.5 ton
Control Mode	Biaxial horizontally
Max. Stroke	+/- 75 mm
Max. Velocity	50 cm/sec
Max. Acceleration	1.0 g
Frequency Range	DC-50Hz

Model soil is Jumoonjin sand, classified as SP by Unified Soil Classification System. Average particle size(D_{50}) is 0.57mm, and Specific gravity(G_s) is 2.62. The detail properties of model soil are summarized in table 3.2. To make loose saturated sand condition, in this research, the water sedimentation method was used. Detail process to make loose sand is as follows. At first, the acryl soil box was filled with water. Then, saturated sand which is soaked overnight is poured into soil box filled with water at constant height. When saturated sand is poured, it should be treated with caution not to be lumped.

Table 3.2 Properties of model soil

Properties	Jumoonjun sand
USCS	SP
Effective grain size, D_{10}	0.38mm
Average particle size, D_{50}	0.57mm
Coefficient of uniformity, C_u	1.58
Specific gravity, G_s	2.62
Maximum dry unit weight, r_{max}	15.99kN/ m^3
Minimum dry unit weight, r_{min}	13.05kN/ m^3

Figure 3.2 shows that schematic drawing of test section and measuring instruments. The height of saturated sand is 50cm and two aluminum model pile which has same length, same diameter, and same properties are installed. In table 3.3, detail properties of aluminum model pile are summarized. Especially, all of model pile in this research has same young's modulus (E) which is 67.82GPa and same length which is 550mm. However, the pile diameters are various such as 14mm, 28mm, and 42mm to evaluate the effect of diameter. The embedded depth of model pile is 50cm, and the model piles are fixed to the bottom of the soil box to simulate rock-socketed pile.
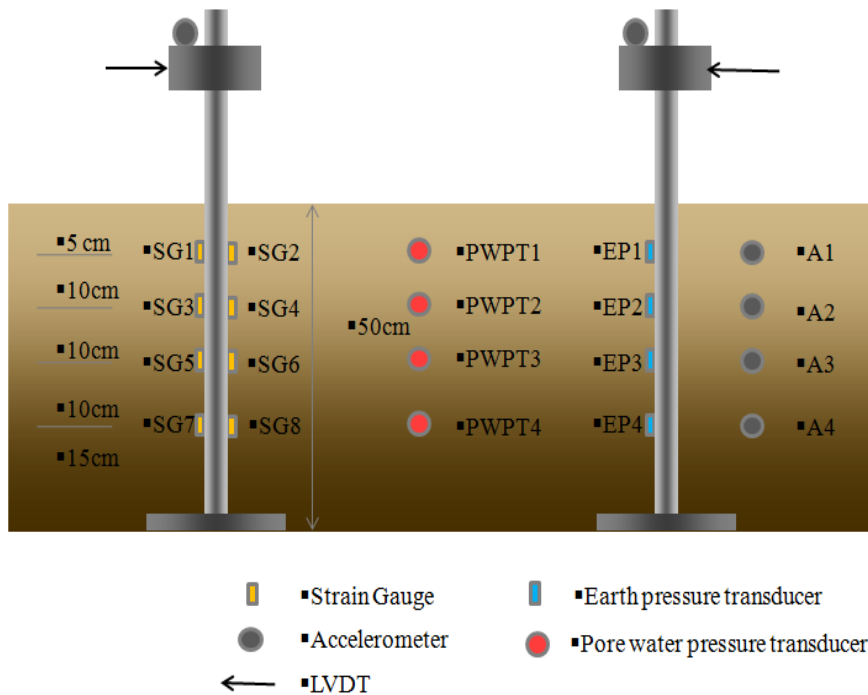
Figure 3.3 Schematic drawing of test section

Table 3.3 Properties of model pile

Properties	Aluminum alloy		
Young's modulus, E	67.82 GPa	67.82 Gpa	67.82 Gpa
Length	550 mm	550mm	550mm
Outside diameter	14 mm	28mm	42mm
Wall Thickness	1 mm	2mm	3mm
EI of the section	58.86 Nm^2	941.74Nm^2	4767.55Nm^2

(a)
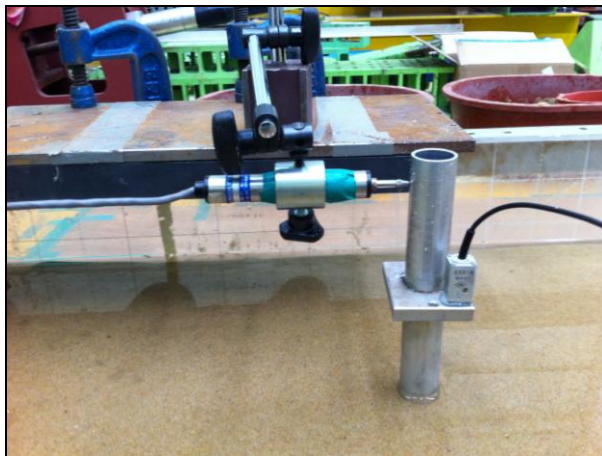
(b)
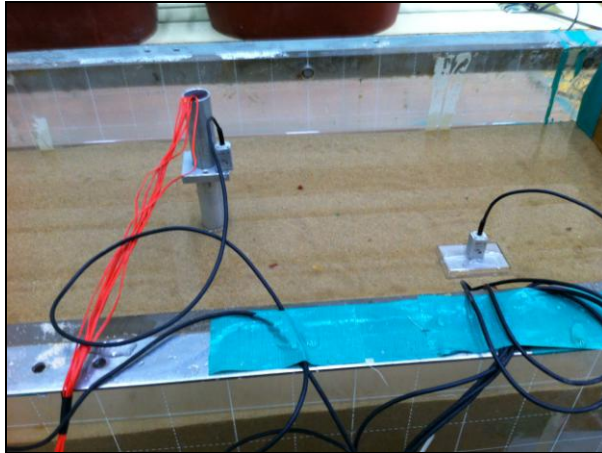
(c)

(d)

Figure 3.4 Panoramic view of test set-up and accelerometer

Five type of measuring instruments are used in this research. First of all, strain gauge is used to estimate strain, and then, moment and pile displacement can be calculated from this data. Accelerometer is used to estimate acceleratio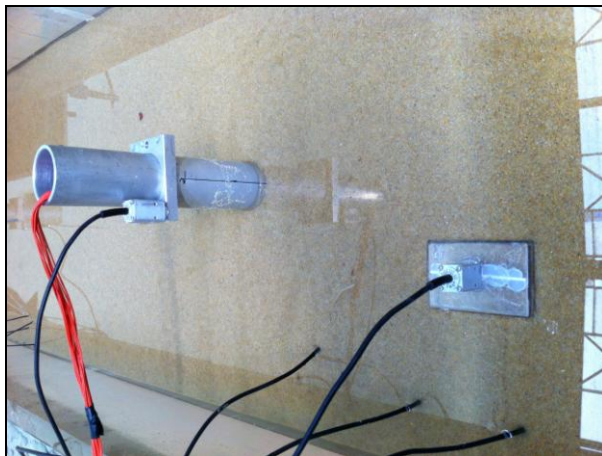n of pile head and ground, and then, the displacement of pile head and ground can be calculated. Moreover, from LVDT, pile displacement can be estimated, from earth pressure transducer, the earth pressure acting on pile can be estimated, and from pore water pressure transducer, pore water pressure which occurred by seismic loading can be estimated. As shown in figure 3.2, accelerometer and LVDT is installed at head of left pile and strain gauges are attached on the body of left pile. Accelerometer and LVDT is also installed at head of right pile and earth pressure transducers are attached on the body of right pile. The reason that same type of measuring instruments (accelerometer and LVDT) is installed at both piles is to prevent from error of estimation by measuring instruments. Moreover, strain gauges are attached on both side of each pile is also to prevent from error of estimation by measuring instruments. Pore water pressure transducers and accelerometers are installed in the ground at the same depth with strain gauge or earth pressure. To install the Pore water pressure transducers and the accelerometers at the exact depth, they are attached on wire in advance, and then, the wire is installed on the bottom of soil box vertically.

Test conditions are shown in Table 3.4. There are Total six test cases; two cases (Case 1-1 and Case 1-2) of these are from Dr. Han's results. The

type of input seismic wave is sine wave, input acceleration is 0.2g, input frequency is 10Hz, and ground relative density is 25% at the each cases. 5cm of sponges are attached at the both side of soil box for prevention from the interference of a reflected wave. There are two type of upper mass which weigh 0kg and 3.8kg, from this condition, it will be analyzed the relation between existence of upper mass and the dynamic earth pressure acting on pile. Moreover, there are three type of pile diameters which are 1.4cm, 2.8cm, and 4.2cm, from this parameter, it will be evaluated the effect of pile diameter to the dynamic earth pressure acting on pile.

Table 3.4 Test program

	Input Acc.	Input frequency	Upper mass	Relative density	Diameter
Case 1-1*	0.2g	10Hz	0 kg	25%	1.4cm
Case 1-2*	0.2g	10Hz	3.8 kg	25%	1.4cm
Case 2-1	0.2g	10Hz	0 kg	25%	2.8cm
Case 2-2	0.2g	10Hz	3.8 kg	25%	2.8cm
Case 3-1	0.2g	10Hz	0 kg	25%	4.2cm
Case 3-2	0.2g	10Hz	3.8 kg	25%	4.2cm

* Han(2006)

Chapter 4 1g shaking table test results

4.1 Earth pressure in saturated sand

As shown in figure 4.1, kim et al.(2004) suggested that dynamic earth pressure acting on quay wall can be divided into fluctuating component and non-fluctuating component. Moreover, Han(2006) suggested that dynamic earth pressure acting on pile foundation can be divided into fluctuating component and non-fluctuating component. In this research, the same analyzing method which dividing earth pressure into two components is used. To divide the dynamic earth pressure acting on pile foundation by fluctuating component and non-fluctuating component, frequency filtering method was used.
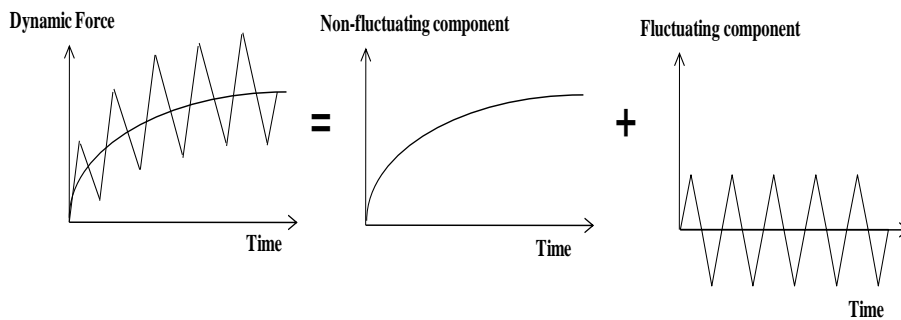

Figure 4.1 Division of fluctuating and non-fluctuating components (Kim et al., 2004)

Figure 4.2 shows that comparison between pore water pressure and dynamic earth pressure acting on pile by dividing into fluctuating component and non-fluctuating component in Case 1-2. In figure 4.2 (c) and figure 4.2 (e), dynamic earth pressure and excess pore pressure has almost same tendency and magnitude in non-fluctuating component. In figure 4.2 (d) and figure 4.2 (f), dynamic earth pressure and excess pore pressure has also almost same tendency and magnitude in fluctuating component. From this result, when the liquefaction is occurred by earthquake, it can be confirm that there are in close relation between dynamic earth pressure and excess pore pressure. Besides, in figure 4.2 (a) and figure 4.2 (c), total dynamic earth pressure and total excess pore pressure are similar to their non-fluctuating component in the tendency and magnitude. It can be also confirmed by comparing between figure 4.2 (b) and figure 4.2 (e). Therefore, most of total dynamic earth pressure and excess pore pressure consist of non-fluctuating component.
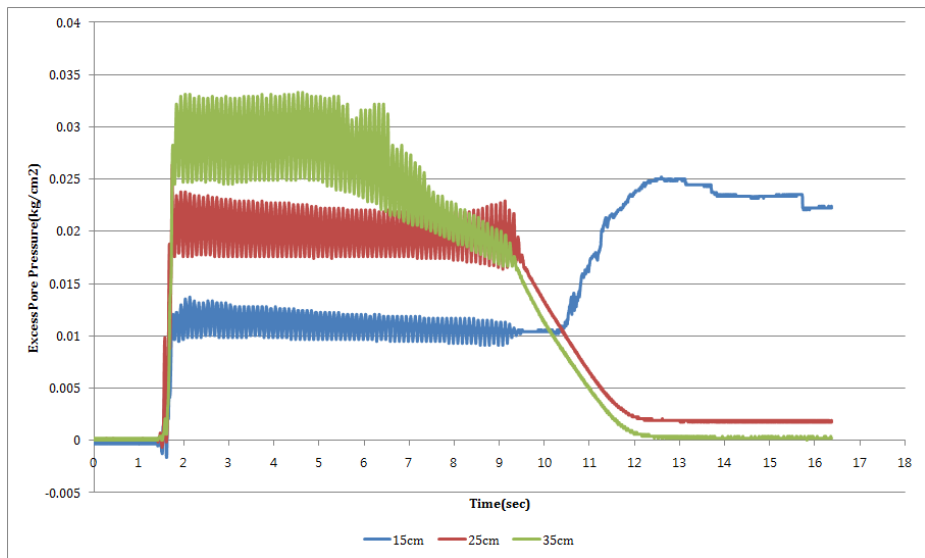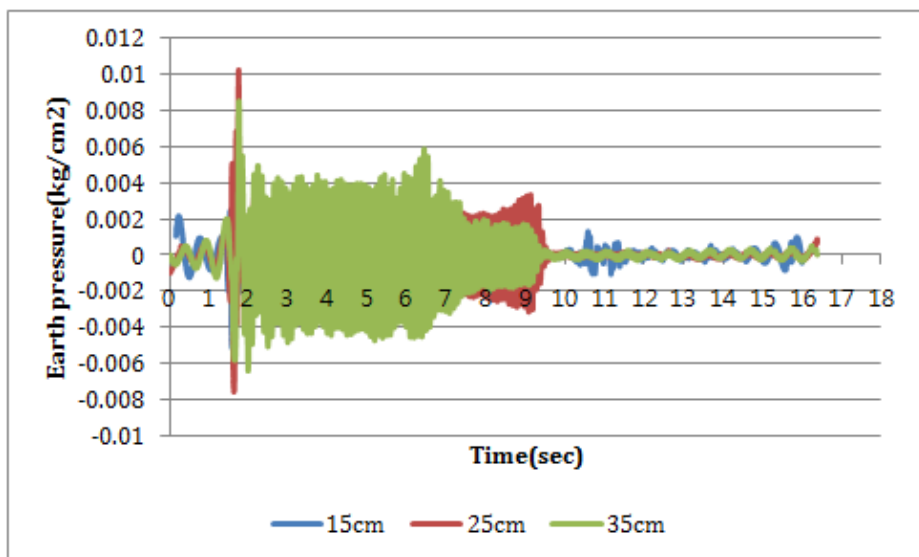
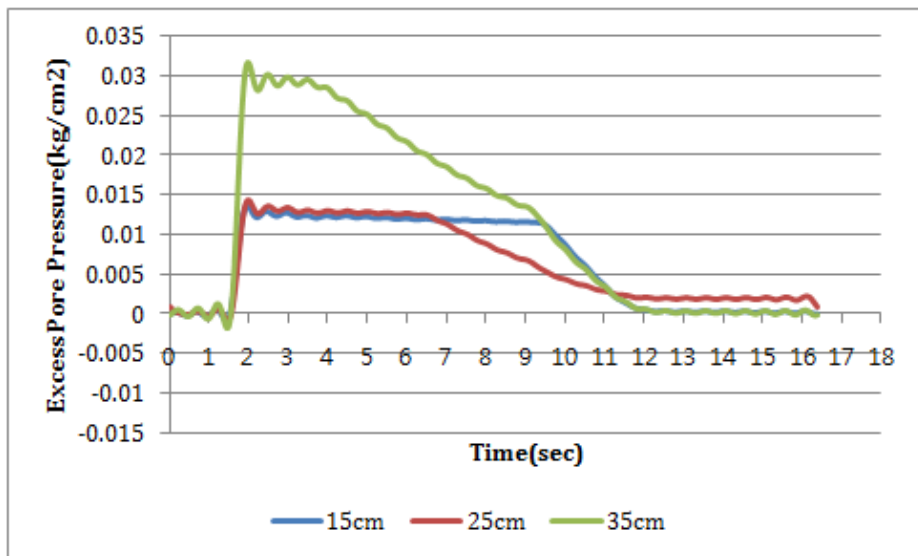(a) Total Earth pressure
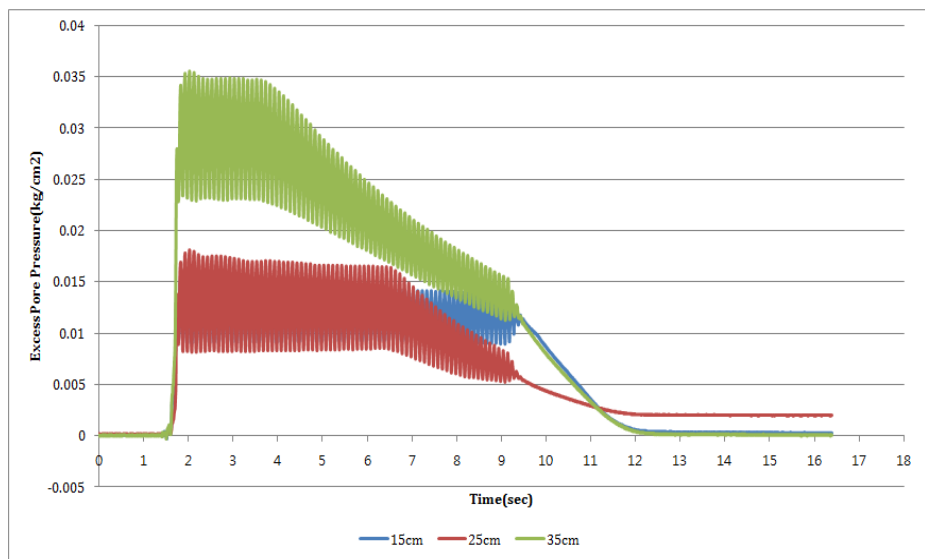
(b) Total excess pore pressure
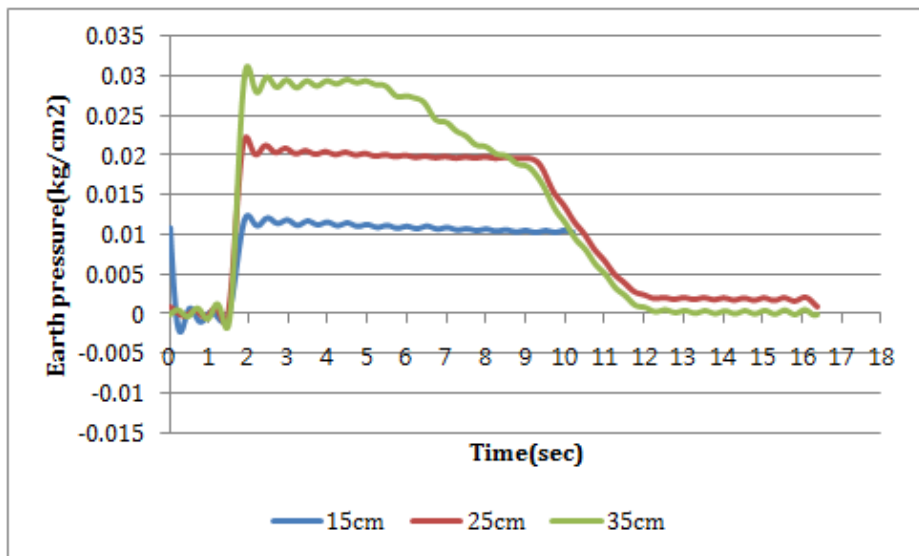
(c) Non-Fluctuating component of Earth pressure

(d) Fluctuating component of Earth pressure

(e) Non-Fluctuating component of Excess pore pressure

(f) Fluctuating component of Excess pore pressure

Figure 4.2 Comparison of Earth pressure and excess pore pressure (Case 1-2)

In figure 4.3, the figure 4.2 (c), (d), (e), (f) are shown again on a large scale for confirming the magnitude easily. From figure 4.3, it can be confirmed again that the almost same tendency and magnitude of dynamic earth pressure and excess pore pressure. However, as shown in figure 4.3 (c), (d), the measuring result of not dynamic earth pressure but excess pore pressure is almost same at the depth of 15cm and 25cm. The reason of this result is thought that the pore water pressure transducer moves up and down when liquefaction was occurred by seismic loading. In other words, it can be inferred that pore water pressure transducer moves other position from original position, by accident, the pore water pressure transducer at the depth of 15cm and 25cm overlapped each other. Therefore, the magnitude of measuring result at the depth of 15cm and 25cm is almost same. When the measuring instruments are installed, the wire was used for preventing this error. However, it can be supposed that the wire cannot resist to the ground displacement by liquefaction.
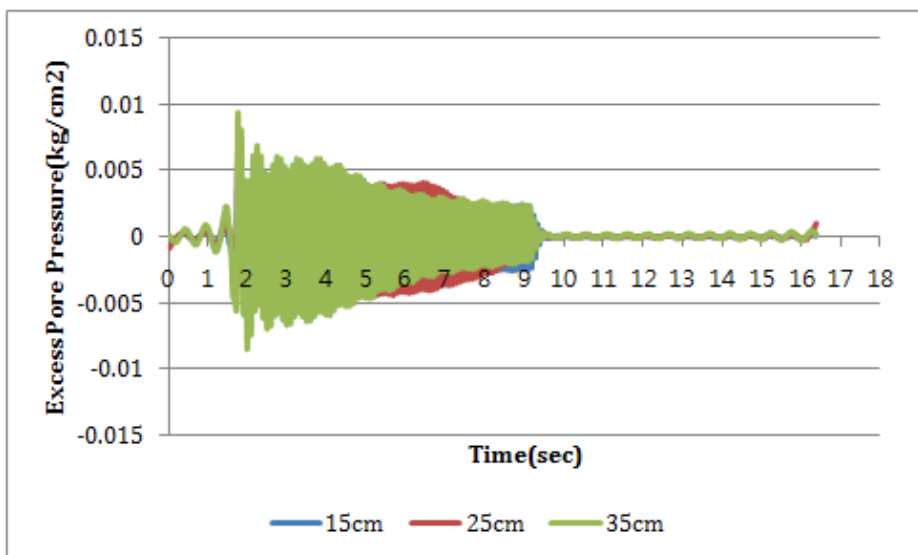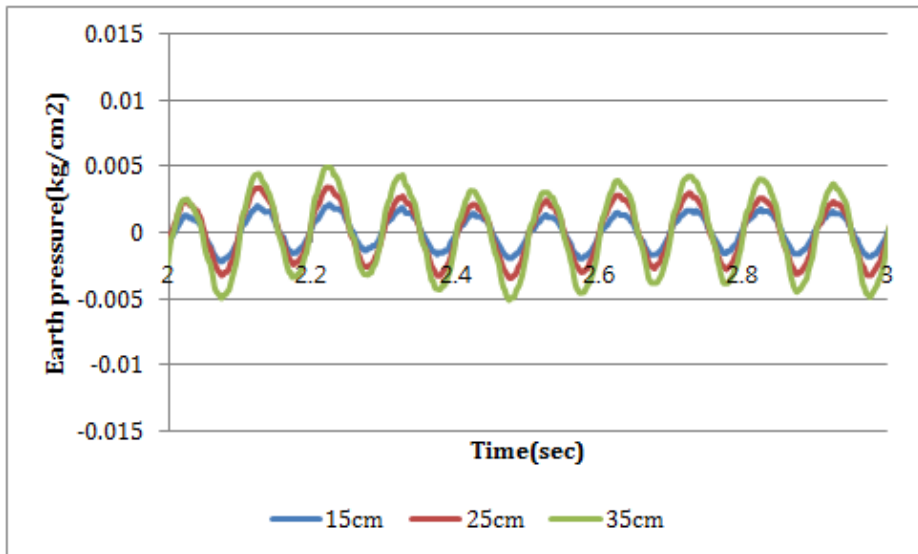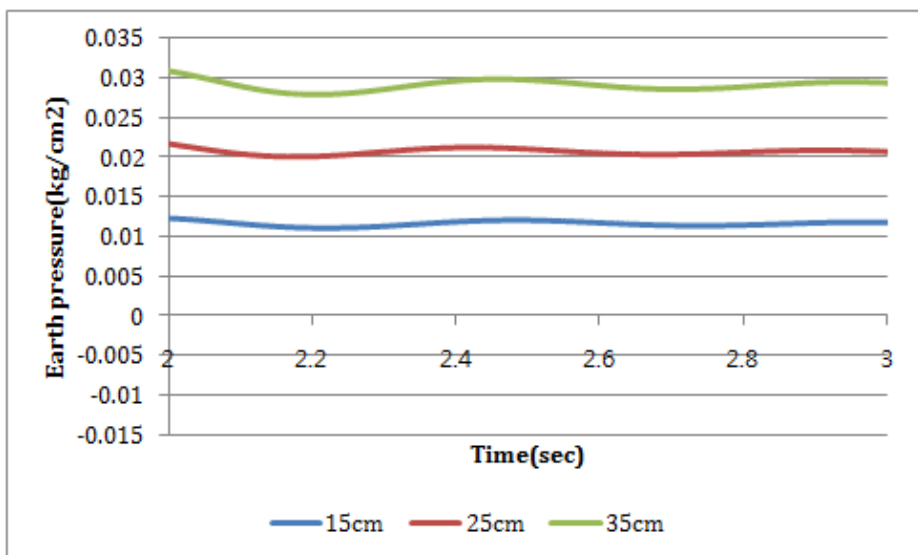
(a) Non-Fluctuating component of Earth pressure

(b) Fluctuating component of Earth pressure

(c) Non-Fluctuating component of Excess pore pressure
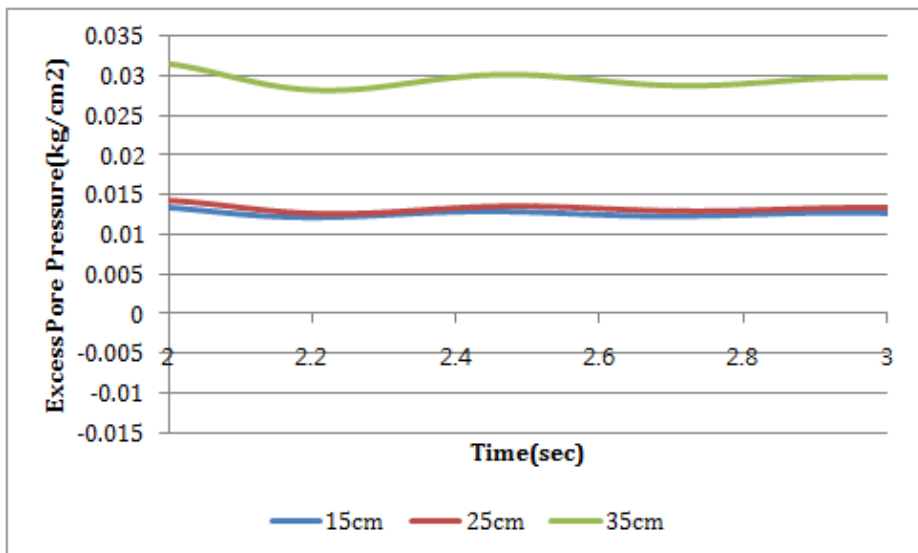
(d) Fluctuating component of Excess pore pressure

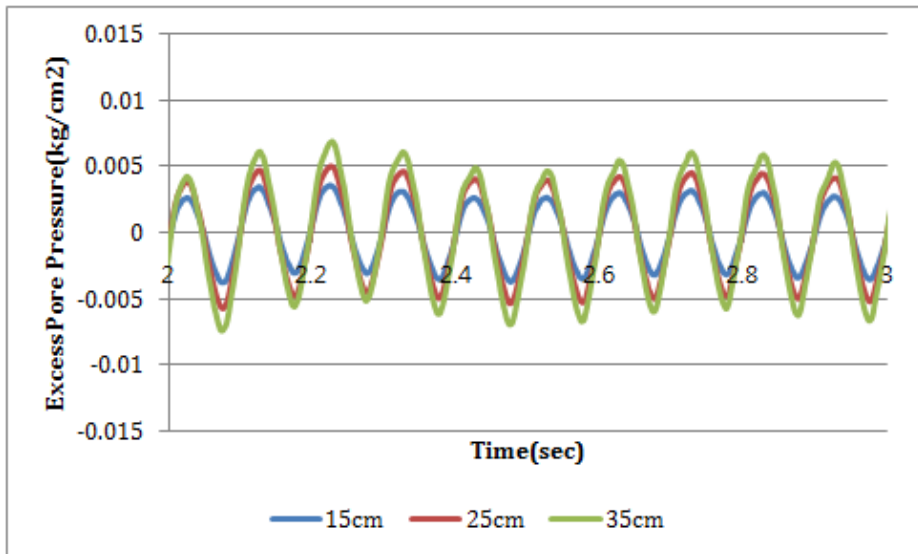Figure 4.3 Comparison of Earth pressure and excess pore pressure (Case1-2, 2sec~3sec)

4.2 Pile displacement according to pile diameter in saturated sand

Figure 4.4 shows that maximum pile displacement according to upper mass with depth in saturated sand. The process of calculating pile displacement with depth is as follows. At first, moment curves can be attained from strain. When extrapolation is conducted, cubic spline method is used. Then pile displacement with depth can be calculated by double integral this moment curve.
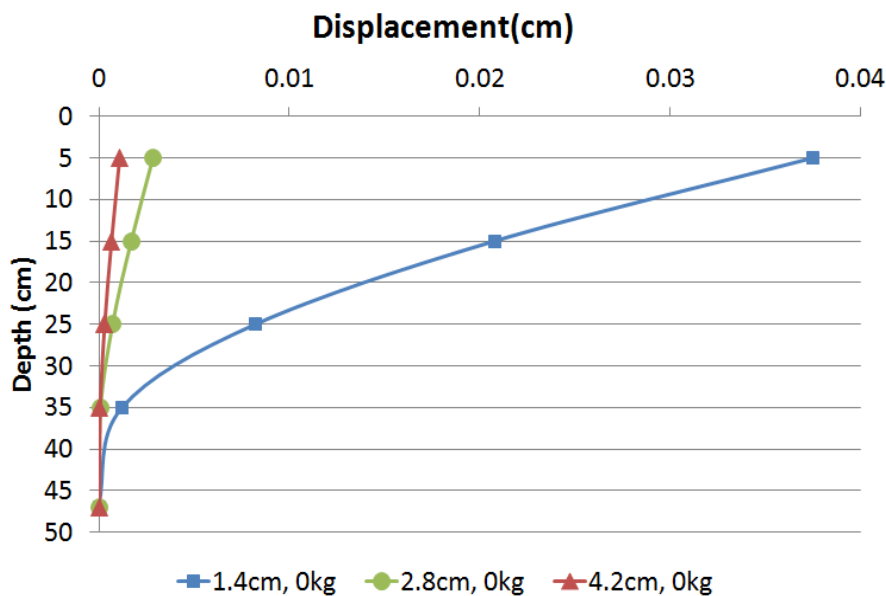
(a) Maximum Displacement, Upper Mass(0kg)
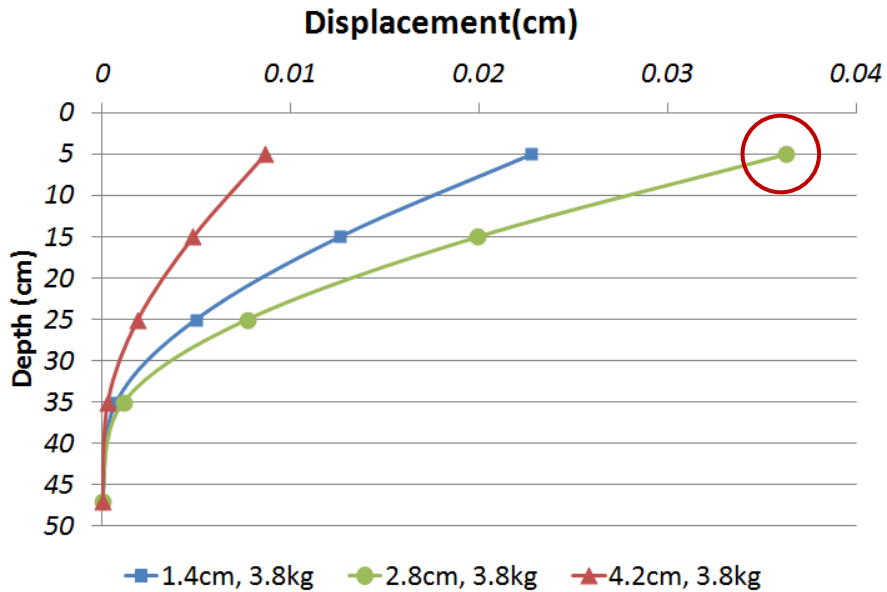
(b) Maximum Displacement, Upper Mass(0kg)

Figure 4.4 Maximum Displacement according to Upper Mass

Figure 4.4 (a) shows that maximum pile displacement with depth without upper mass. As shown in this figure, the maximum pile displacement decreases as pile diameter increases. It is because that pile stiffness decreases as pile diameter decreases. In other words, in case that the pile stiffness is smaller, the pile can be bent easily, whereas in case that the pile stiffness is larger, the pile can have larger resistance. Therefore, in case that the pile stiffness is larger, the maximum pile displacement is smaller. However, figure 4.4 (b) shows a little different result from figure 4.4 (a). In figure 4.4 (b), Case 2-2 shows the largest pile displacement, and this result cannot explain by the effect of pile stiffness. Therefore, Fast Fourier Transform Analysis is

conducted to analyze this tendency.

Fast Fourier Transform Analysis is the method that time signal is transformed into frequency signal. Figure 4.5 shows that the result of Fast Fourier Transform Analysis which analyzed Sweep Test in each Cases. The analysis is conducted with Case 2-2, 3-2 because that the Case 2-2 is in case of having upper mass, therefore, FFT analysis is conducted with all case of having upper mass. However, when Case 1-2 was conducted at the past by Han, sweep test was not conducted. So in this research, Fast Fourier Transform Analysis of this Case 1-2 could not be conducted and could not be compared with other Cases. Figure 4.5 shows that acceleration ratio with frequency. In Case 2-2, the amplitude increases at about 18Hz, in Case 3-2, the amplitude increases at about 45Hz. In other words, in Case 2-2, the amplitude increases at the lower frequency than Case 3-2. In this research, the input frequency is 10Hz, Therefore the frequency of Case 2-2 which have increase of amplitude is closer to input frequency than Case 3-2. It is inferred that the larger maximum pile displacement was occurred from these reason.
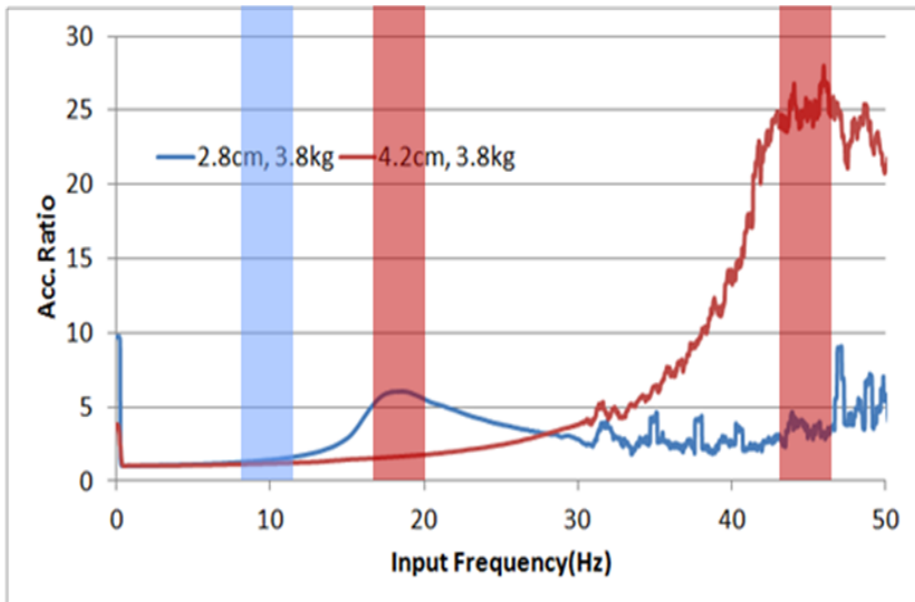
Figure 4.5 Acceleration Ratio with Input Frequency

4.3 Earth pressure according to pile diameter in saturated sand

Figure 4.6 shows that the maximum earth pressure acting on pile according to the existence of upper mass with depth in saturated sand. As shown in figure 4.6 (a), the maximum earth pressure acting on pile having various diameters without upper mass shows the triangle distribution which increases as the depth increases. This triangle distribution is because that the effect of liquefaction by seismic loading. When the liquefaction is occurred in saturated sand, the ground looses the confining pressure, so the ground behaves like fluid. Therefore the liquefied ground has triangle distribution like fluid. Moreover, it can be confirmed that the pile diameter don't have any influence on the magnitude and distribution of the maximum earth pressure. From this result, in case without upper mass, it can be concluded that there are no relation between maximum earth pressures acting on pile and the pile diameters.

As shown in figure 4.6 (b), when there are the upper mass on the pile head, the maximum earth pressure acting on pile having various diameters also shows the triangle distribution which increases as the depth increases. This triangle distribution is also because that the effect of liquefaction by seismic loading Moreover, when there are the upper mass on the pile head, it can be also confirmed that the pile diameter don't have any influence on the magnitude and distribution of the maximum earth pressure. From this result, in case of having upper mass, it can be concluded that there are no relation

between maximum earth pressure acting on pile and the pile diameters.

However, the result of Case 2-2 is different from other Cases, this result can be explained by the result of Fast Fourier Transform Analysis. In other words, the frequency of Case 2-2 which has increase of amplitude is closer to input frequency than Case 3-2. It is inferred that the larger maximum earth pressure was occurred from these reason.
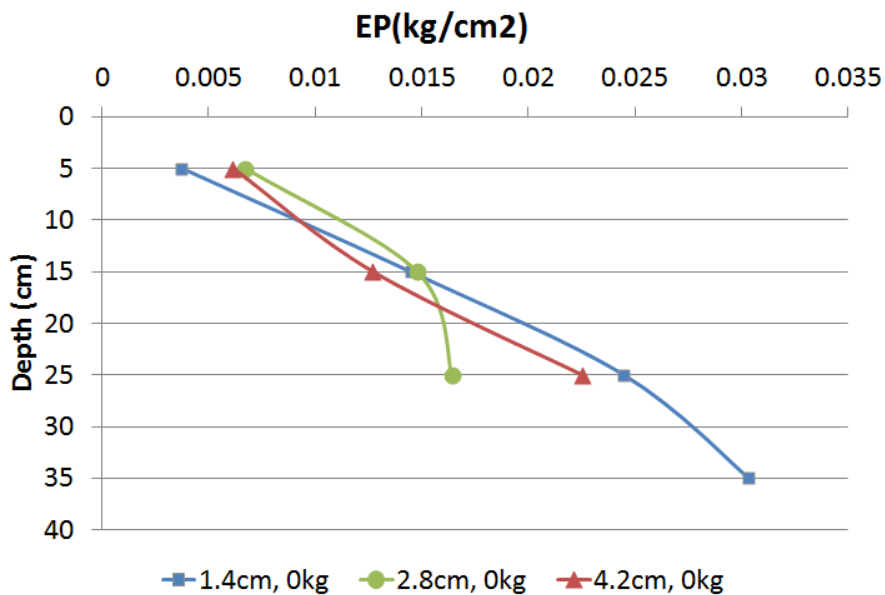
(a) Maximum Earth Pressure, Upper Mass(0kg)
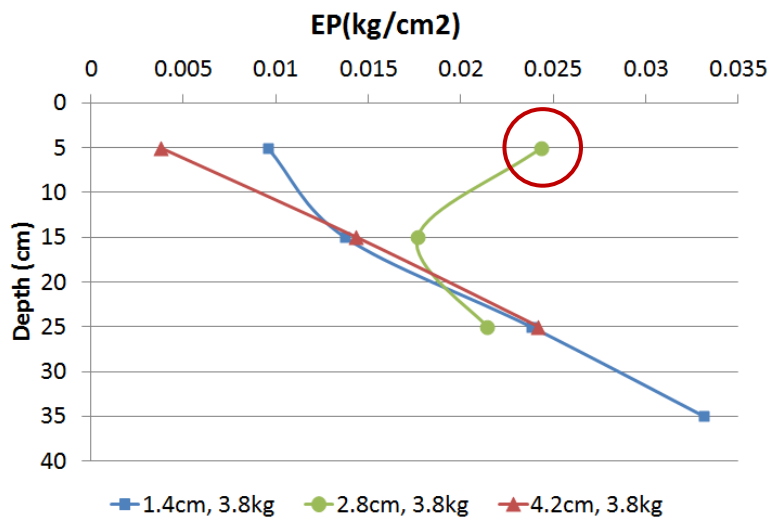
(b) Maximum Earth Pressure, Upper Mass(3.8kg)

Figure 4.6 Maximum Earth Pressure according to Upper Mass

4.4 Comparison of Inertial effect and kinematic effect

Force components acting on soil-pile-structure in earthquake can be divided into inertial force and kinematic force. In this research, the upper mass represent inertial force and ground displacement represent kinematic force. Therefore, it can be confirmed that the effect of inertial force by the existence of upper mass, and the effect of kinematic force by ground displacement in liquefied ground.

Figure 4.7 shows that the maximum earth pressure according to existence of upper mass and pile diameters with depth. In Chaper 4.3, it was confirmed that there are no relation between pile diameter and maximum earth pressure acting on pile. Moreover, from figure 4.7, it can be also confirmed that the magnitude and distribution of maximum earth pressure acting on pile with depth, irrespective of upper mass. The existence of upper mass is important factor to evaluate the effect of inertial force, therefore the inertial force by upper mass have no influence on the maximum earth pressure acting on pile with depth.
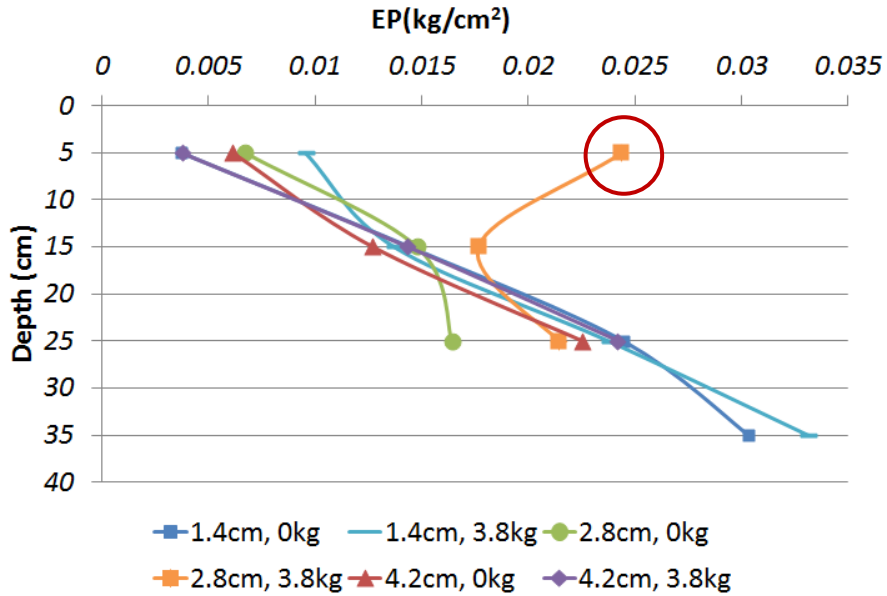
Figure 4.7 Maximum Earth Pressure according to Pile diameter and Upper mass

Figure 4.8 shows that maximum ground displacement in liquefied sand. Because that the liquefaction is representative non-linear behavior, there are lots of errors of measuring instruments such as moving up and down of measuring instrument. Therefore, the data which relatively estimate the ground displacement are used in this research (Case 1-1, 1-2, 2-2). To measure the ground displacement, accelerometer was used. The maximum ground displacement can be calculated by double integral data which were attained from accelerometer.

As shown in figure 4.8, the maximum ground displacements don't have the accurate tendency. However, the maximum ground displacements increase as the depth increase or have a fixed distribution as the depth

increase. These tendencies are similar to the tendency of maximum earth pressure which increases with depth, therefore, it can be confirmed that the ground displacements have influence on the maximum earth pressure acting on pile. In other words, the maximum earth pressure acting on pile have more influence on kinematic force than inertial force, therefore, kinematic effect is the dominant factor on the maximum earth pressure acting on pile

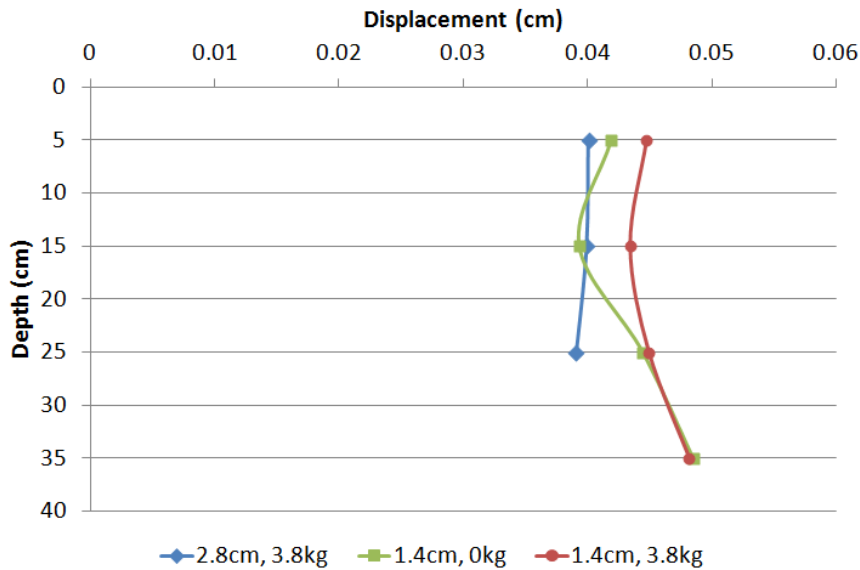Figure 4.8 Maximum Ground displacements according to Pile diameter and Upper mass

Chapter 5 Evaluation of Fluctuation Component of Earth pressure

5.1 Westergaard Solution

Equation (1) is Westergaard Solution suggested by Westergaard for calculating dynamic water pressure acting on dam or quay wall (Westergaard, 1933). Kohama and Sato suggested that modified Westergaard solution which use γ_{sat} (2000) like equation (2) for calculating the dynamic earth pressure acting on quay wall in liquefied ground. Because of the behavior of liquefied ground like fluid, when the dynamic earth pressure is calculated by using modified Westergaard solution, γ_{sat} will replace γ_w in the equation (Kohama, 2000; Sato, 2000; Fujiwara, 2000; Kim, 2004). Moreover, Han suggested that the equation (2) can be used to calculate the dynamic earth pressure acting on not only quay wall or dam but also pile foundations (2006). When this equation (2) is used to calculate the dynamic earth pressure acting on pile foundation, a shape factor is applied because that the shape of pile foundation is not a plane surface but a curved surface. Therefore, the dynamic earth pressure acting on pile foundation can be estimated by 30% of Westergaard solution using γ_{sat} or 50% of Westergaard solution using γ_w (Han, 2006). In this research, the applicability of the Westergaard solution for calculating the dynamic earth pressure acting on pile foundation will be

verified based on additional parametric study.

$$q(z) = \frac{7}{8} k_h \gamma_w \sqrt{H_w z}$$

$$F_{FWD} = \int q(z) = \frac{7}{12} k_h \gamma_w H_w^2$$

(1)

where, $q(z)$: dynamic water pressure at the depth of z

F_{FWD} : fluctuating component of dynamic water force acting on front of wall

γ_w : unit weight of water

k_h : horizontal seismic coefficient

H_w : water depth

$$q(z) = \frac{7}{8} k_h \gamma_{sat} \sqrt{H_w z}$$

$$F_{DF} = \int q(z) = \frac{7}{12} k_h \gamma_{sat} H_w^2$$

(2)

where,

F_{DF} : fluctuating component of dynamic thrust after liquefaction

γ_{sat} : saturated unit weight of soil

5.2 Comparison of Dynamic earth pressures and Westergaard solution

In figure 5.1, the graph shows that the comparison between fluctuating components of dynamic earth pressure acting on pile foundation in the experimental case of only kinematic force applied without upper load and the analytical method by Westergaard solution. As shown in figure 5.1, flucuating component of maximum earth pressure with depth have similar magnitude and similar distribution according to various pile diameter. Moreover, it can be confirmed that the result of Westergaard solution using γ_w (equation (1)) and result of Westergaard solution using γ_{sat} (equation (2)) are very similar to their magnitude and distribution. Then, it can be concluded that fluctuating component of the maximum dynamic earth pressure with depth acting on pile foundation in liquefied ground is able to be calculated by 50% of Westergaard solution using γ_w or 25% of Westergaard solution using γ_{sat}. This conclusion almost corresponds with the result of Han (2006) which concluded that fluctuating component of the maximum dynamic earth pressure with depth acting on pile foundation in liquefied ground is able to be calculated by 50% of Westergaard solution using γ_w or 29% of Westergaard solution using γ_{sat}. Therefore, It can be verified that fluctuating component of the maximum dynamic earth pressure with depth acting on pile foundation in liquefied

ground is able to be calculated by Westergaard solution and it has no correlation with pile diameters.
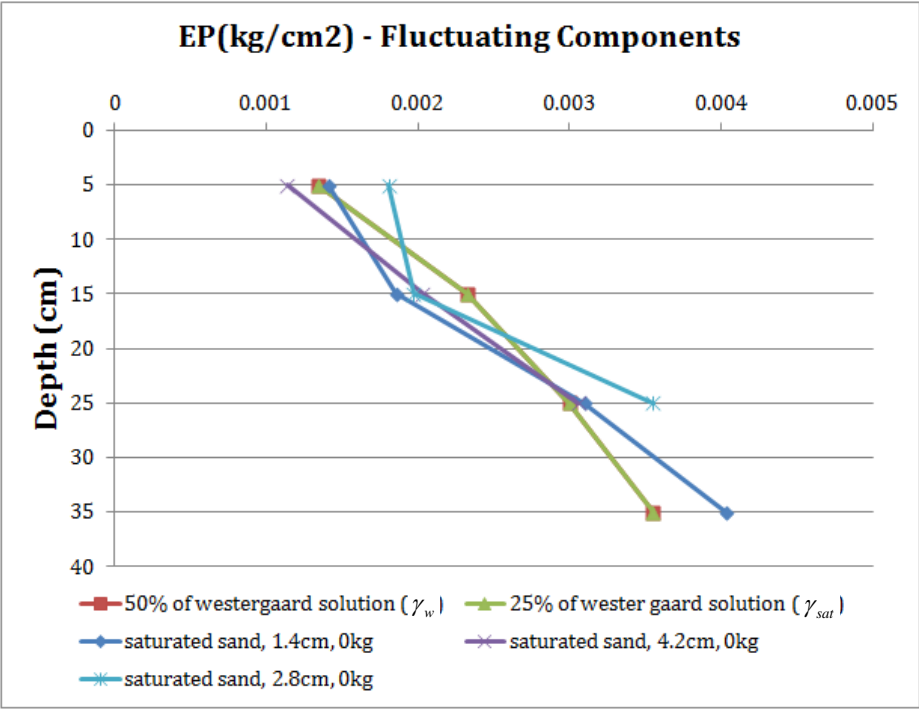

Figure 5.1 Dynamic earth pressures vs. Westergaard solution

Chapter 6 Conclusions

In this research, To evaluate earth pressure acting on pile during liquefaction and to analyze the dynamic behavior of the pile in liquefiable soils, 1g shaking table test was conducted. Following conclusions were drawn by experimental researches.

When liquefaction was occurred, saturated sand behave as cohesive liquid. Therefore, earth pressure acting on piles increases with depth in liquefiable soil and its distribution is similar to pore water pressure. Moreover, earth pressure acting on piles was almost same for various pile diameters.

Concentrated mass on piles head have no influence on earth pressure acting on piles, whereas ground displacement have important effect on earth pressure in liquefiable soil. Thus, it is concluded that the kinematic effect is dominant factor in the earth pressure compared to the inertial effect.

The westergaard solution which can calculate the fluctuating component of the dynamic water pressure acting on quay wall and its modified equation which can calculate the fluctuating component of the dynamic earth pressure acting on quay wall were compared with the shaking table test results. It was confirmed that the fluctuating component of earth pressure was able to calculate by 50% of westergaard solution using γ_w.

Moreover, It was also able to calculate by 25% of westergaard solution using

γ_{sat} .

Bibliography

Dou, H. and Byrne, P. (1996). "Dynamic Response of Single Piles and Soil-Pile Interaction," Can. Geotech. J., 33(1), 80-96.

Fujiwara, T., Horikoshi, K., Higuchi, Y., and Sueoka, T. (2000). "Estimation of Dynamic Displacement of Gravity Type Quay Walls based on Centrifuge Modeling," Proc. Of 12th World Conf. on Earthquake Engrg., The New Zealand Society for Earthquake Engrg., Upper Hutt, New Zealand, Paper No. 2429.

Han, J.T. (2006). "Evaluation of Seismic Behavior of Piles in Liquefiable Ground by Shaking Table Tests", Ph. D. Dissertation, Seoul National University, Korea.

Kim, S.R. (2003). "Evaluation of Seismic Behavior of Gravity Type Quay Wall by Shaking Table Tests," Ph. D. Dissertation, Seoul National University, Korea.

Kohama, E. (2000). "A Study on the Stability of Gravity Type Quay Wall during Earthquake," Ph. D. Dissertation, Hokkaido University, Japan.

Liu, L. and Dobry, R. (1995). "Effect of liquefaction on lateral response of piles by centrifuge model tests," National Center for Earthquake Engineering

Research (NCEER) Bulletin, 9(1), January, 7-11.

Sato, M., Watanabe, H., Takeda, T., and Shimada, M. (2000). "Simplified Method to Evaluate Caisson Type Quay Wall Movement," Proc. Of 12th World Conf. on Earthquake Engrg., The New Zealand Society for Earthquake Engrg., Upper Hutt, New Zealand, Paper No. 1440.

Tokimatsu, K., Suzuki, H., Sato, M. (2005). " Effects of inertial and kinematic interaction on seismic behavior of pile with embedded foundation," Soil Dynamics and Earthquake Engineering 25 (2005) 753-762.

Westergaard, H.M. (1933). "Water Pressures on Dams during Earthquakes," Trans. Of ASCE vol. 98, 418-432.

초   록

본 연구에서는 액상화 가능지반에서 말뚝에 작용하는 동적 토압을 1g 진동대 실험을 통해 평가하고자 하였다. 말뚝 변위의 절대적인 크기와 분포를 다양한 말뚝의 직경과 상부질량의 유무에 차이를 두며 분석 하였다. 액상화 가능 지반에서 말뚝에 작용하는 깊이 별 동적 토압 역시 말뚝의 직경과 상부질량의 조건을 달리하며 분석하였다. 또한, 다양한 상부질량 조건에서 말뚝에 작용하는 깊이 별 동적 토압을 지반의 변위와 비교 분석하였다. 이와 같이 다양한 변수에 대한 연구를 수행한 결과 말뚝의 직경과 상부질량의 존재의 유무는 말뚝에 작용하는 동적 토압의 크기와 분포에 큰 영향을 주지 못한다는 것을 확인하였다.

상부질량의 유무는 관성 효과를 대표하고, 액상화로 인한 지반의 변위는 운동학적 효과를 대표한다고 할 수 있다. 따라서 상부질량의 조건과 지반의 변위를 비교하여 관성 효과와 운동학적 효과를 정성적으로 비교 분석하였다. 관성 효과와 운동학적 효과를 비교 분석한 결과, 말뚝에 작용하는 동적 토압에 영향을 주는 주요 요소로는 관성 효과보다 운동학적 효과가 더 지배적인 요소라는 것을 확인할 수 있었다.

안벽 구조물에 작용하는 동적 수압을 산정하기 위해 고안된 westergaard의 해는 안벽 구조물에 작용하는 동적 토압을 산정하기 위한 식으로 수정하여 쓰일 수 있다. 이 식을 안벽 구조물이 아닌 말뚝 기초에 작용하는 동적 토압의 진동성분을 산정하기 위한 식으로 이용하는 방법이 제안되었고, 이를 검증하여 액상화 지반에서 말뚝기초에 작용하는 동적 토압의 진동성분을 산술적으로 구할 수 있도록 하고자 한다.